Heritability of visual cortex architecture and perception

Ivan Alvarez[1,2], Nonie J. Finlayson[3,4], Shwe Ei[3,5], Benjamin de Haas[3,6], John A. Greenwood[3] & D. Samuel Schwarzkopf[3,7]*

[1] Helen Wills Neuroscience Institute, University of California, Berkeley, USA

[2] Wellcome Centre for Integrative Neuroimaging, University of Oxford, United Kingdom

[3] Experimental Psychology, University College London, United Kingdom

[4] Ipsos, Brisbane, Queensland, Australia

[5] GKT School of Medical Education, Kings College London, UK

[6] Department of Psychology, Justus-Liebig University, Giessen, Germany

[7] School of Optometry & Vision Science, University of Auckland, New Zealand

* Correspondence:

Dr. D. S. Schwarzkopf
Associate Professor
School of Optometry & Vision Science
Faculty of Medical & Health Sciences
University of Auckland
Private Bag 92019
Auckland 1142
New Zealand

Email: s.schwarzkopf@auckland.ac.nz
Phone: +64 9 373 7599

Keywords: visual perception, size perception, twin study, heritability, population receptive fields, Human Connectome Project

Abstract

How much of our visual processing, and thus our visual perception, is inherited? Variations in perceptual judgments of the size of visual objects have been found to correlate with idiosyncratic differences in the spatial sensitivity of primary visual cortex. Here we tested their heritability using retinotopic mapping and psychophysical experiments on size perception. The spatial sensitivity of human visual cortex, quantified by population receptive field analysis, was more similar in monozygotic (MZ) than dizygotic (DZ) twin pairs, especially in extrastriate regions, suggesting a partial genetic determination. Furthermore, inter-individual differences in perceptual bias for size judgments – how large or small stimuli appear to an observer – showed considerable heritability. This contrasts with previously reported idiosyncrasies across visual field quadrants, which showed little evidence of heritability. Our findings are therefore consistent with heritability of broad, eccentricity-dependent properties of visual function and cortical architecture, while quadrant-specific idiosyncrasies appear to lack a genetic basis.

Introduction

Human visual perception shows striking individual differences. Face recognition abilities vary from 'face blindness' through to 'super-recognisers'[1], and two individuals can look at the same object and see vastly different colours[2]. The appearance of visual objects also varies idiosyncratically across different retinal locations[3–6]. For example, for a simple judgement of object size, one individual may perceive objects as particularly small in the upper-left visual field, while another perceives it as small in the lower-right visual field. Biases for perceiving object size correlate with individual cortical surface area and spatial tuning properties of primary visual cortex (V1)[5–7]. The extent to which these variations in size perception and associated cortical architecture are heritable is currently unknown.

Twin studies provide a unique opportunity to study environmental and genetic factors for such inter- and intra-individual differences in visual system architecture and perception. The genetic proportion of observed variation between humans is defined as heritability[8,9], which is distinct from environmental influences, shared or unique. Identical (MZ) twins share 100% of their genes, whereas non-identical (DZ) twins share 50% on average. Classical twin designs compare correlations between MZ and DZ twin pairs to isolate how much variance in a variable of interest can be attributed to genetic versus environmental components[9].

Previous research has shown that relatively complex aspects of visual perception, such as binocular rivalry[10], bistable perception[11] and face recognition ability[12,13] all have a heritable factor. Heritability is also evident in related aspects of cortical function. A study using magnetoencephalography showed that visually-induced gamma oscillations in early visual cortex are heritable[14]. We and others have reported links between gamma peak frequency, occipital levels of the neurotransmitter *gamma*-Aminobutyric acid (GABA)[15] and the functional architecture of early visual cortex[16–18] (but see also[19]). Considering these links, the heritability of gamma oscillations could therefore reflect the heritability of the functional properties of human visual cortex, such as its basic architecture and spatial selectivity.

Here, we set out to understand how much of the organization of human visual cortex could be explained by genetic factors. We first examined broad characteristics of the functional

architecture of early visual cortex by conducting retinotopic mapping experiments with functional magnetic resonance imaging (fMRI). Specifically, each participant underwent three 8-minute runs of fMRI in which they viewed stimuli combining a rotating wedge with expanding or contracting rings[20], and we then used population receptive field (pRF) analysis[5,21] to estimate the preferred visual field location and spatial selectivity of each voxel in visual cortex. We found the organization of retinotopic maps, especially in the extrastriate cortex, more similar in MZ than DZ twin pairs. This heritability is lower in striate cortex (V1), in particular with regard to spatial selectivity and cortical magnification. The size of visual regions was found to be heritable including V1, a finding that we replicate in a larger database obtained from the Human Connectome Project.

To understand if this cortical heritability has consequences for simple perceptual judgements, we also measured psychophysical biases in size perception. We found that individual differences in overall peripheral perceptual biases were heritable. We also measured their variation across visual quadrants and replicate our previous finding of a link between these biases and cortical idiosyncrasies in the spatial selectivity of visual cortex[5]. We found no evidence for heritability in these variations for either size judgements, or for their neural correlates in pRF size estimates. Although broad aspects of cortical architecture and perception are heritable, their idiosyncratic pattern across the visual field is not.

Results

Monozygotic visual field maps are qualitatively more similar than dizygotic maps

We first consider the heritability of broad characteristics of the retinotopic maps in early visual areas. Figure 1 shows example cortical visual field maps from one MZ twin pair and one DZ twin pair. To generate a qualitative measure of the overall similarity of visual field maps between twin pairs at the broadest scale, we obtained similarity ratings from six naïve raters. These raters had expertise in delineating retinotopic maps (experience ranging from several months to years), but had never seen these data before. Each rater was given a slideshow showing polar angle maps displayed on spherical models of cortical hemispheres (see Figure 1).

Each twin pair was presented side by side, from a comparable viewpoint, and at the same goodness-of-fit threshold (R^2>0.05). Raters were instructed to rate how similar they judged the maps from each pair to be, on a scale of 0 (zero similarities) to 10 (identical). Raters were asked to ignore the spatial extent of cortical activity, the camera orientation, and differences in local noise, as these would likely result from technical or analytical artifacts. Raters were blind to the genetic status of the twin pairs. Similarity ratings were significantly higher (paired t-test, t(64)=3.65, p=0.0005) between MZ twins (M = 6.14) than between DZ twins (M = 5.04). This suggests that twins with higher shared genetic background have a higher degree of similarity in the topological organisation of visual cortex.

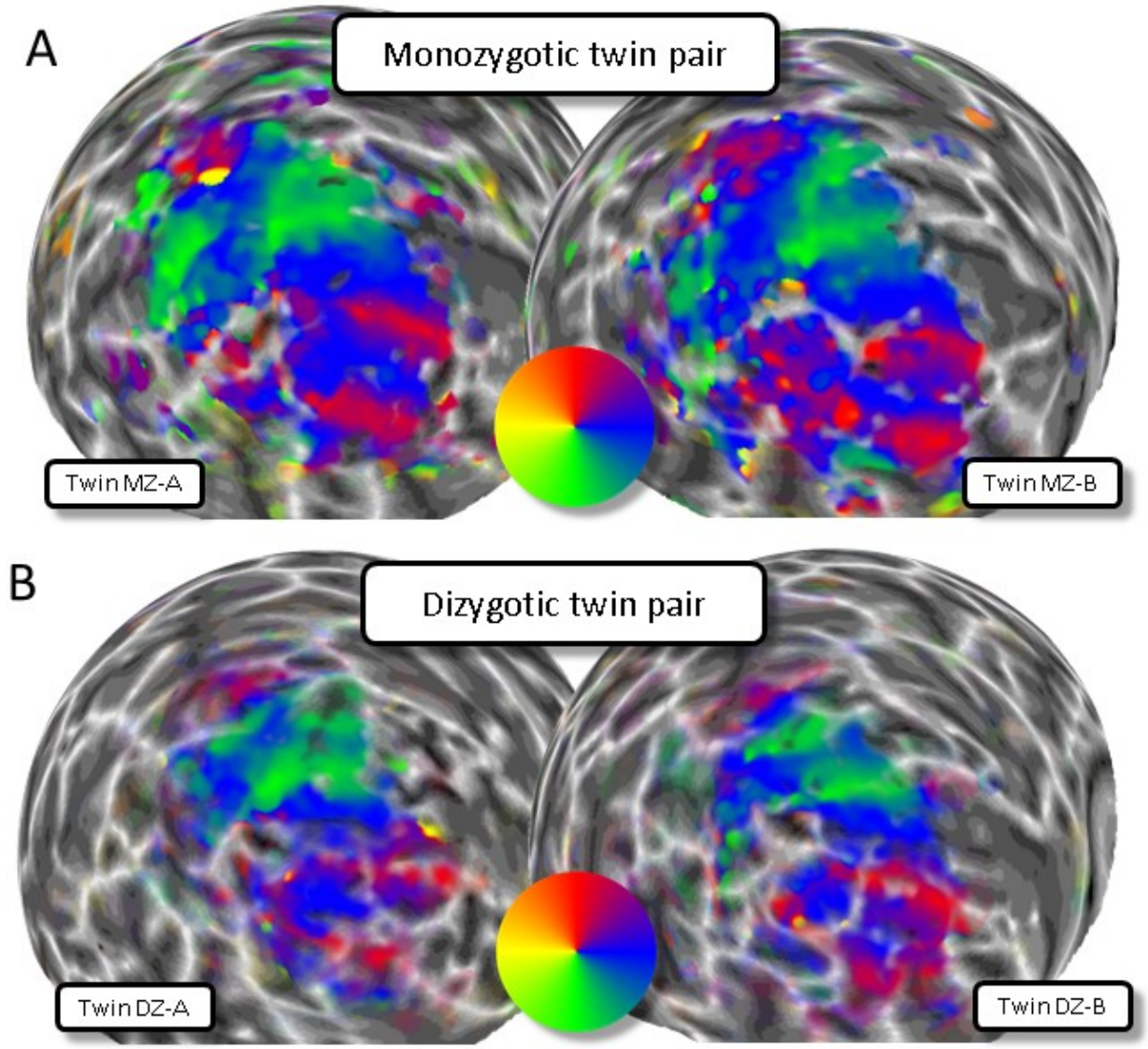

Figure 1. *A-B.* Retinotopic polar angle maps for an identical MZ (A) and a non-identical DZ twin pair (B). Polar angle maps are shown on an inflated spherical model of the cortical surface for the left hemisphere only. Each plot shows data from one individual. Greyscale indicates the cortical curvature, with darker patches corresponding to sulci, and lighter patches corresponding to gyri. The pseudo-color code (see insets) denotes the preferred polar angle in the visual field for a voxel at a given cortical location, as derived from population receptive field (pRF) analysis.

Surface area of early visual regions is heritable

We next examined the heritability of cortical surface area in visual regions. Previous research has also suggested correlations between the macroscopic surface area of visual regions and perceptual or cognitive functions[6,7,22–25]. We first examined the heritability of the surface area of whole cortical regions. Measuring the surface area of each cortical region based on manual delineation of the retinotopic map, however, is limited to the mapped region of the visual field and dependent on the accuracy of, and selection criteria applied by, the individual rater creating the delineation. In order to avoid such biases, we opted for a fully automated procedure for quantifying regional surface area. We used a probabilistic technique that uses spatial normalization of each participant's cortical surface model to a common template to predict the retinotopic organization of V1-V3 based on previously acquired reference maps[26]. We then quantified the surface area for each these regions, expressed as a percentage of total cortical area.

Once we obtained the region delineations, we correlated cortical surface area measures between twins. This analysis divides the twins in each pair into two groups, A and B, and then calculates the correlation between these groups. Because group assignment is arbitrary, we first carried out a permutation analysis, reassigning twins in each pair randomly to group A and B, and then calculated the correlation. We performed 10,000 permutations and calculated the median correlation across permutations as the representative measure of similarity between the two parameters. Figure 2A shows the intra-class correlations and scatter plots for individual twin pairs for each visual region. The surface areas in MZ twins were positively correlated in region V1 (r_{MZ}=0.64, p=0.0033), V2 (r_{MZ}=0.83, $p<10^{-5}$), and V3 (r_{MZ}=0.81, $p<10^{-4}$). In contrast, correlations in DZ twins were not statistically significant (V1: r_{DZ}=-0.26, p=0.3683; V2: r_{DZ}=0.16, p=0.5824; V3: r_{DZ}=0.23, p=0.4397). Based on Falconer's formula[9] these correlations suggest very high heritability for cortical surface area in all three visual regions (H^2>100%).

One caveat in this analysis is the relatively small sample size for between-subject comparisons. This is evidenced by the large confidence intervals, and it is particularly noticeable for the results from V1 in the DZ group, where correlations were negative, which is a statistical artifact. To supplement this analysis, we replicated the probabilistic analysis of cortical area in a

much larger, independent data set provided by the Human Connectome Project[27,28]. We performed the equivalent analysis on cortical reconstructions of 138 MZ and 79 DZ twin pairs and found a qualitatively similar pattern of results (Figure 2B). Correlations in MZ twins were numerically greater for regions V1-V3 (V1: r_{MZ}=0.87, $p<10^{-41}$; V2: r_{MZ}=0.71, $p<10^{-21}$; V3: r_{MZ}=0.67, $p<10^{-18}$) than those for DZ twins (V1: r_{DZ}=0.62, $p<10^{-8}$; V2: r_{DZ}=0.3, p=0.0067; V3: r_{DZ}=0.29, p=0.0085). The HCP dataset showed a lower heritability estimate for V1 (H^2=49%), when compared to V2 (H^2=81%) and V3 (H^2=75%). As the plot of intra-class correlations shows (Figure 2B), results for V2 and V3 were consistent with additive genetic factors, while correlations for V1 fell between that model and the unity line, suggesting a weaker genetic influence than in the extrastriate regions.

As an additional level of analyses, we repeated the correlation analysis for absolute, rather than relative, surface area (mm^2) for visual regions in our original twin sample. The results were consistent with those for relative surface areas (Supplementary Figure S1). As previous research suggested that overall brain structure is heritable[29], we tested the intra-class correlations for the surface area of the whole cortex (Supplementary Figure S2). Cortical area was correlated in both twin groups (MZ: r_{MZ}=0.9, $p<10^{-6}$; DZ: r_{DZ}=0.8, p=0.0006), with stronger correlation in MZ twins, confirming modest heritability of overall surface area (H^2=20%). We also replicated this finding in the Human Connectome Project data set (MZ: r_{MZ}=0.95, $p<10^{-71}$; DZ: r_{DZ}=0.74, $p<10^{-13}$), with a greater heritability estimate (H^2=43%), possibly driven by the more precise estimate of correlations in a larger sample size.

Across two independent datasets, our findings converge to suggest that both the relative and absolute surface areas of visual regions V1, V2 and V3 are largely determined by additive genetic factors.

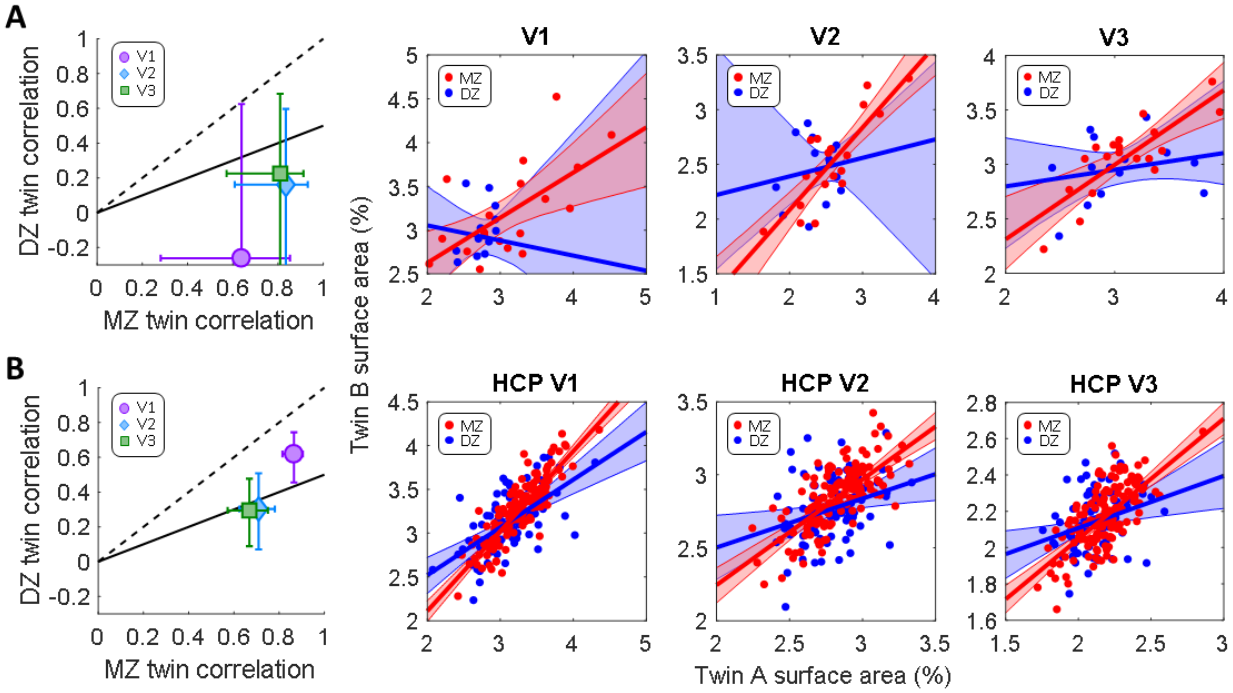

Figure 2. *Left column:* Intra-class correlations between DZ twins plotted against that for MZ twins for surface areas expressed as a percentage of overall cortical area. Visual regions were defined based on a probabilistic anatomical procedure. Data are shown for areas V1 (purple disc), V2 (blue diamond), and V3 (green square). Error bars denote 95% confidence intervals based on bootstrapping. The dotted line indicates the expected correlation if a measure is only determined by shared environmental factors, the solid line if the expected correlation is determined by additive genetic factors. *Other columns:* Relative cortical surface area for regions V1-V3 for the two twins in each pair separately for the MZ (red points) and DZ (blue points) groups. Each point denotes data from one twin pair. Solid lines indicate linear regression fits for each group, and the shaded regions denote their 95% confidence intervals based on bootstrapping. A. Data from our novel sample of participants. B. Replication data from the Human Connectome Project (HCP).

Average size perception biases are heritable

Our brain imaging data is consistent with genetic determination of the functional architecture of human visual cortex in a broad, macroscopic scale. We next examine how the macroscopic scale relate to visual perceptual processing.

We recently introduced a method for efficiently measuring each individual's *biases* in the apparent size of simple circle stimuli presented parafoveally[5,30]. In each trial of this task, participants view small circular test stimuli of variable sizes, one per visual field quadrant, and judge which stimulus was the same size as a centrally presented reference of constant size

(Figure 3A). This technique produces reliable estimates of perceptual biases[30,31]. As a measure of objective task performance, this method also estimates discrimination *uncertainty* – the range of stimulus sizes across which participants judged the test stimulus to appear to be the same size as the reference. We tested the overall level of heritability of these perceptual measures. We quantified the average size perception bias across four stimulus locations for each participant, and correlated them with the corresponding average bias from fellow twins. This analysis is equivalent to that for macroscopic surface areas of individual visual regions discussed above, including the permutation procedure.

The average subjective perceptual bias across the four quadrants (Figure 3B, also shown with individual points in Figure 3C) was significantly correlated between MZ twin pairs (r_{MZ}=0.52, p=0.014) but not between DZ twins (r_{DZ}=0.08, p=0.7777). One DZ participant showed an unusually strong perceptual bias of -0.265, with a Mahalanobis distance of >10 from the bivariate group mean. Removal of this outlier did not alter the results in a substantive manner (r_{DZ}=0.07, p=0.8314).

In contrast, sensitivity, as quantified by discrimination uncertainty (Figures 3B and 3D), was correlated for both groups of twins to a similar extent, albeit non-significantly (r_{MZ}=0.41, p=0.0612; r_{DZ}=0.38, p=0.1797). The equivalent correlations in MZ and DZ groups indicate that overall differences in this objective ability are not heritable (H^2=5%). In contrast, perceptual bias, the *subjective* appearance of the stimulus size, was determined in large part by additive genetic factors (H^2=87%).

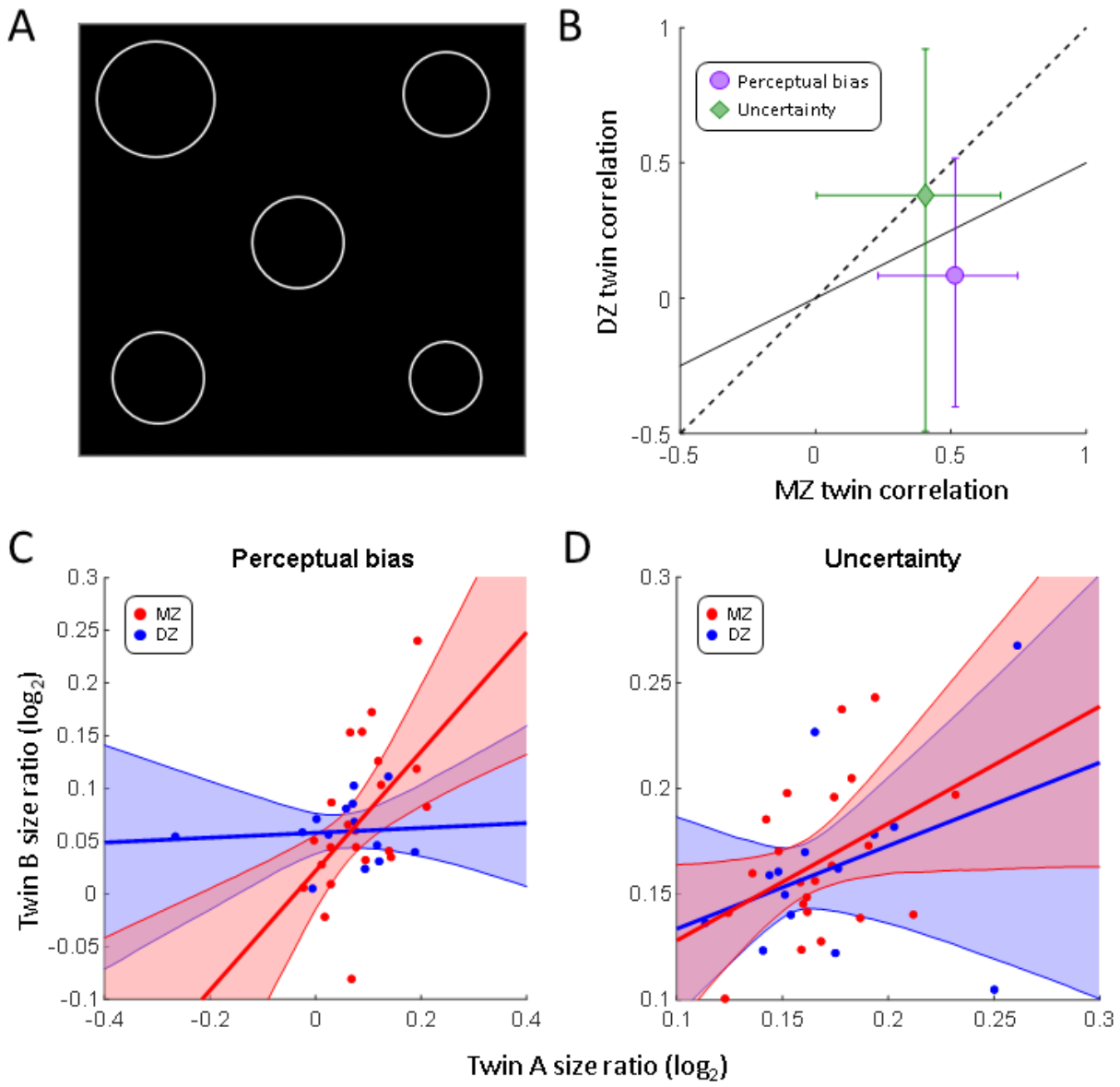

Figure 3. A. A typical stimulus array in the psychophysical task to measure perceptual biases in size judgments. Observers were instructed to fixate on a dot at the center of the screen and judge which of the four circles in the quadrants was the same size as the central reference circle (here, the lower left). B. Intra-class correlations for DZ twins plotted against MZ twins for perceptual bias (purple disc) and discrimination uncertainty (green diamond) averaged across visual field quadrants. Error bars denote 95% confidence intervals based on bootstrapping. The lines indicate theoretical predictions; the dashed line indicates the expected correlation if a measure is only determined by environmental factors, and the solid line indicates the expected correlation if a measure is determined by additive genetic factors. C-D. Perceptual bias (C) and uncertainty (D) averaged across visual field quadrants for the two twins in each pair separately for the MZ (red points) and DZ (blue points) groups. Each point denotes data from one twin pair. Solid lines indicate linear regression fits for each group, and the shaded regions denote their 95% confidence intervals based on bootstrapping.

Map architecture is more heritable in extrastriate regions

For added sensitivity and understanding the heritability of functional architecture of visual cortex, we next conducted more fine-grained analyses. We quantified the degree of similarity in the *spatial distribution* of polar angle and eccentricity preferences, as well as pRF sizes and cortical magnification separately for each visual region. This allowed us to examine the individual heritability of these pRF properties for each twin pair and then calculate the average heritability at the group level. To this end, we used spatially-normalized surface maps for each participant generated by cortical alignment to a common template. We calculated an average retinotopic map across all participants irrespective of twin status, and manually delineated visual regions V1, V2 and V3 based on this average map. As a measure of similarity for each twin pair and brain region, we calculated the correlation of each of the 4 pRF properties across all retinotopically responsive vertices in a given delineated region. Retinotopically responsive vertices were defined as vertices which surpassed a statistical threshold of $R^2>0.1$ in the pRF analysis for both twins in the pair. We calculated the average correlation in each group and determined the heritability using Falconer's formula[9].

Figure 4 shows the average heritability for the four pRF properties and the three visual regions V1-V3. For polar angle and pRF size, heritability appeared to gradually increase across the visual hierarchy, while we did not observe the same pattern for eccentricity or cortical magnification. To test statistically whether heritability differed between visual regions for any of these measures, we bootstrapped the group means for MZ and DZ twins 10,000 times by resampling twin pairs with replacement, and then recalculated the heritability for each visual region for each bootstrap iteration. We then fit a linear regression to the heritability across the three regions V1-V3 for each iteration and finally determined the proportion of this bootstrap distribution of regression slopes that were ≤0. This showed that heritability for polar angle significantly ($p=0.0008$) increased across the visual hierarchy. For the other measures this effect was not significant (eccentricity: $p=0.8809$; pRF size: $p=0.0714$; CMF: $p=0.4292$).

To determine the one-tailed statistical significance level of the heritability for each region and pRF property, we quantified the proportion of bootstrap iterations in which heritability was ≤0. This showed that in V3 the heritability was significantly greater than zero for polar angle ($p<0.0001$) and pRF size ($p<0.0001$). In V2 it was significant only for eccentricity ($p=0.0019$). None of the other tests survived Bonferroni correction for multiple comparisons (all other comparisons $p\geq0.0111$; $\alpha=0.0042$).

Altogether, the overall tendency for MZ correlations to be larger than DZ correlations suggests that broad variations in the spatial response properties of visual cortex are heritable, particularly in extrastriate region V3 for polar angle preferences and pRF size.

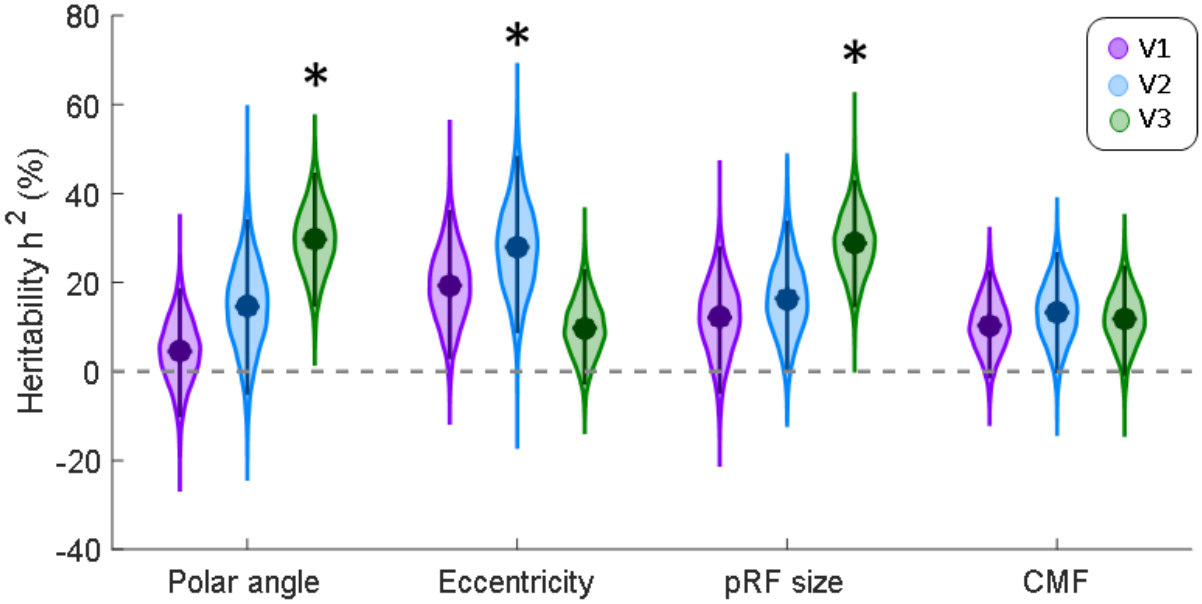

Figure 4. Heritability for population receptive field parameters in each visual region. Data are shown for polar angle, eccentricity, pRF size, and cortical magnification factor (CMF) parameters, as derived from pRF analysis. Filled circles indicate the group means. The violin plot shows the bootstrap distribution for each pRF property and visual region, and the error bars denote its 95% confidence intervals. Asterisks indicate significant differences at $p<0.05$, after Bonferroni correction for multiple tests.

Quadrant-specific patterns of perceptual biases correlate with pRF size

Our recent work showed that perceptual biases for judgements of object size are correlated with pRF size in corresponding parts of V1[5]. In visual field locations where perceptual biases are stronger, such that people perceive a circular test stimulus to be smaller than the

reference stimulus, the corresponding pRFs at that location are larger. Are such idiosyncrasies in cortical function and perception genetically determined?

To answer this question, we tested whether the correlation between perceptual biases and pRFs replicates in this new sample. Our fMRI measurements allowed us to focus on the parts of V1 corresponding to our stimulus locations. For each participant and quadrant, we determined the average pRF size at cortical locations that corresponded to the eccentricity of stimuli in the psychophysical experiment (see Methods and our previous work[5] for a complete description of the analysis).

We then calculated the correlation between perceptual biases and pRF size. For this analysis, we pooled data irrespective of twin status because this correlation should occur independently in each individual. This analysis replicated our previous results: the average correlation between V1 pRF sizes and perceptual biases across the whole sample was r_{μ}=0.25, which was significantly greater than zero (t(65)=2.53, p=0.0137). That is, participants tended to underestimate the size of visual stimuli at locations where pRFs were larger. The equivalent analysis showed that discrimination *uncertainty* was not significantly correlated with pRF size (r_{μ}=-0.21, t(65)=-1.81, p=0.0752).

Quadrant-specific idiosyncrasies in pRF size are not strongly heritable

To examine the heritability of these quadrant-specific idiosyncrasies in pRF size, we considered variations in pRF size selectively for the parts of visual cortex responsive to our psychophysical stimulus locations. As above, for each visual region, we determined the pRF size at the eccentricity of our stimuli in each visual-field quadrant. We calculated the correlation in pRF sizes across the four quadrants in each visual region for each twin pair. As above, we used average correlation and bootstrapping to determine if heritability was statistically greater than zero and if it changed across the visual hierarchy.

Heritability for quadrant-specific pRF size (Supplementary Figure S3) did not change significantly across the visual hierarchy (p=0.9461). Moreover, heritability was not significantly greater than zero in any visual region (V1: p=0.2733; V2: p=0.441; V3: p=0.9486). This finding differs from the above region-wise analysis where we found that heritability of pRF significantly

increased across the visual hierarchy and was significant for V3 as a whole (Figure 4). This could suggest that the overall pattern of pRF sizes across V3 is heritable, but the fine-grained pattern of pRF sizes across quadrants is not. Alternatively, heritability may simply be more difficult to ascertain with the reduction in data required to examine selected parts of these visual regions.

Quadrant-specific patterns of perceptual biases are not heritable

Equivalent analyses allowed us to test the heritability for idiosyncratic patterns of psychophysical measurements in MZ and DZ twin pairs. That is, separately for each twin pair we calculated the correlation between the four perceptual biases measured for each quadrant, and then determined the heritability using bootstrapping as described earlier. We have recently shown relatively strong test-retest reliability of such patterns within individual observers[5,30]. In spite of this, heritability for perceptual bias (p=0.225) and discrimination uncertainty (p=0.1695) was not significantly greater than zero (Supplementary Figure S4). This suggests, the variation of these perceptual measures within individuals is not genetically determined.

Discussion

We carried out fMRI and behavioral measures on identical and non-identical twin pairs to probe the genetic components for the functional architecture of early visual cortex and subjective size perception. Our neuroimaging findings showed a moderate genetic component for the general architecture of retinotopic maps, most notably for polar angle preferences and pRF size in extrastriate region V3. Additionally, our findings suggest that the anatomical surface area of early visual regions has a strong genetic component. This was found in both our novel sample of MZ and DZ twins, and in a replication dataset from the Human Connectome Project[27,28]. In this latter dataset, the genetic contribution increased through the cortical hierarchy from V1 to V3. Our findings on the cortical architecture and overall surface area converge to suggest that heritability may be greater for extrastriate cortex.

Heritability in the visual system was not limited to cortical architecture. In a behavioral experiment, we found that individual biases in size perception averaged across the visual field

were more strongly correlated in identical twins than non-identical twins. This was not solely explained by variations in task performance, as we found no evidence of heritability for objective discrimination ability in our participants. Rather, our finding suggests that the factors that drive these overall size perception biases are in a large part driven by genetics.

Interestingly, the same heritability was not evident for the spatial pattern of individual differences in psychophysical measures across quadrants. We previously reported that spatial heterogeneity in perception correlates with the corresponding heterogeneity in pRF sizes in V1[5]. In other words, biases in size perception are more pronounced in locations where pRFs are larger. Here we replicated this relationship in our sample, but found no evidence of strong heritability of these idiosyncrasies, neither for pRF size nor for perceptual biases measured psychophysically. Taken together with the lack of heritability for pRF sizes in V1, these findings suggest that such spatial patterns are in large part driven by non-genetic, experience-dependent factors. It should be noted that correlations between twins for pRF sizes were relatively strong for both MZ and DZ groups. The patterns of pRF sizes may therefore reflect commonalities across participants related to radial asymmetries in pRF size across the visual field reported previously[31].

The probabilistic atlas approach we leveraged for identifying retinotopic regions[26] exploits a close correspondence between cortical curvature and retinotopic maps[32], and it has been posited that the constraints placed on intra-cortical connections due to map organization could determine cortical folding[33]. This hints at the interesting possibility that the genetic component in retinotopic map development may also drive cortical folding, but this hypothesis will need to be tested explicitly in future research.

Taken together, we found that the general architecture of the early visual cortex is highly heritable. The architecture and the spatial selectivity of V3 and higher extrastriate regions may also be more heritable than those of earlier regions. In contrast, the development of quadrant-specific cortical idiosyncrasies in spatial selectivity could be dependent on shared environmental factors. Similar visual experiences during development, for example the visual tasks twins perform or the exposure to urban versus rural settings, could result in differences in spatial selectivity for particular parts of the visual field. They could however also simply be

related to asymmetries in spatial selectivity that most people have in common[31]. Our findings thus converge to suggest that overall biases in size perception are heritable, but their heterogeneity across the visual field is not. Spatial perceptual heterogeneity instead seems determined either by experience-dependent factors or random fluctuations.

Methods

Participants

We collected data from 36 pairs of same-sex twins. All participants were healthy and had normal or corrected-to-normal visual acuity. Participants were financially compensated for their time and travel costs. We obtained written informed consent from all participants and all procedures were approved by the University College London Research Ethics Committee.

Monozygotic (MZ). We recruited 22 pairs of monozygotic (MZ) twins (18 female, 4 male), mean age 25.1 years (18-47 years). Fifteen pairs were right-handed, one pair was left-handed, six pairs were mixed (one twin right-handed, one left-handed). fMRI data from three MZ pairs was excluded: one pair was excluded due to an incidental neurological finding in one twin, with two pairs excluded due to excessive head movement during scanning. All analyses presented here used the remaining 19 MZ pairs.

Dizygotic (DZ). We recruited 14 pairs of dizygotic (DZ) twins (10 female, 4 male), mean age 25.0 years (18-40 years). Thirteen pairs were right-handed, and one pair was left-handed. All DZ twins are included in the analyses presented here.

In addition, data from 217 twin pairs were used as a replication dataset. Data were provided by the Human Connectome Project[27] S1200 release (release date 01-03-2017). We selected participants who met the following criteria; each twin pair had (1) confirmed MZ or DZ status via genetic testing, (2) a complete 3T MRI structural imaging protocol, and (3) data processed to generate cortical surface reconstructions[28]. In total, there were 138 MZ pairs and 79 DZ pairs who met the criteria.

Behavioral experiment

General psychophysical procedures

Participants were seated in a dark, noise-shielded room in front of an LCD monitor (Samsung SyncMaster 2233RZ, resolution: 1680 × 1050, refresh rate: 120Hz). Minimum and maximum luminance values were 0.25 and 230 cd/m^2, and viewing distance was 48cm,

stabilized by means of a chin rest. Participants used both hands to indicate responses by pressing buttons on a keyboard, and stimuli were generated and displayed using MATLAB (MathWorks) and the Psychophysics Toolbox 3[34,35].

Size perception task

To estimate size perception biases efficiency at four visual field locations, we used the Multiple Alternative Perceptual Search procedure (MAPS[5,30]). This task estimates the points of subjective equality between test stimuli across multiple visual field locations and a foveal reference, and can also be used to calculate a general peripheral size bias.

Stimuli. Five light gray (54 cd/m^2) circle outlines were presented against a black background on each trial. One, the *reference*, was presented in the center of the screen and was constant in size (diameter: 0.98°). The remaining four *test stimuli* varied in size from trial to trial, and were presented at the four diagonal polar angles (eccentricity: 3.92°). The test-circle sizes were drawn from a Gaussian distribution centered on the size of the *reference* circle (standard deviation: 0.3 binary log units). One of these four test circles was randomly assigned as the correct *target*, with its size set to be equal to the reference (0 log units difference).

Procedure. Each trial started with a white fixation dot for 500 ms (diameter: 0.2°). The presentation of the stimulus array followed for 200 ms, after which the screen returned to the fixation-only screen. Participants made their responses by pressing the F, V, K, or M key on the keyboard, corresponding to whichever of the four *test stimuli* appeared most similar in size to the *reference*. The experiment was broken up into 20 blocks of 20 trials, with a rest after each block.

Analysis. To estimate perceptual biases for each individual, we fit a model to predict a given participant's behavioral response in each trial (for further details, see[30]). This estimates four perceptual bias (point of subjective equality) parameters for each participant, as well as four uncertainty (discrimination sensitivity) parameters. For the analysis of the overall bias or uncertainty, respectively, we averaged the four bias or uncertainty parameters to obtain one value for each participant.

Questionnaire

Participants were also asked to complete a questionnaire to provide information about environmental factors in their upbringing, such as how often they shared school classes and friends, dressed alike as children, and how often they keep in contact with their twin. In addition to self-report of zygosity from the twins (Question 2), this questionnaire included two questions previously validated to classify twin zygosity with 95% accuracy[36]:

During childhood, were you and your twin as alike as 'two peas in a pod' or were you of ordinary family likeness? (Question 3)
Were you and your twin so similar in appearance at school age that people had difficulty in telling you apart? (Question 4)

Demographics and questionnaire responses. Self-report of twin zygosity originally led to 17 MZ and 19 DZ pairs of twins. The questionnaire results found conflicting categorizations, where the questionnaire criteria zygosity for some twin pairs conflicted with self-reported zygosity. Five DZ pairs disagreed on both criteria (Questions 3 *and* 4), and three DZ and two MZ pairs disagreed on one criterion (Question 3 *or* 4). These 10 twin pairs were contacted and asked if they would take a genetic test through a third-party company (NorthGene, UK). Seven of the eight DZ pairs took the test, and of those, genetic testing found that the five who disagreed on both criteria were (probable) MZ twins. The two (of three) DZ pairs who disagreed on one criterion were both DZ pairs. None of the MZ twin pairs took the genetic test. We consequently switched the categories for the DZ twins whose genetic testing indicated they were MZ twins, leaving us with 22 MZ and 14 DZ twin pairs.

<u>Functional MRI experiment</u>

Parameters

Imaging data were collected on a Siemens Avanto 1.5T MRI scanner located at the Birkbeck-UCL Centre for NeuroImaging, using a 32-channel head coil with the two coils in the middle of the top half of the head coil restricting vision removed, leaving 30 channels. Functional data were acquired with a T2*-weighted multiband 2D echo-planar sequence (2.3

mm isotropic voxels, 36 slices, FOV = 96×96 voxels, TR = 1s, TE = 55ms, acceleration factor = 4). Slices were oriented to maximize coverage of occipital cortex, generally approximately parallel to the calcarine sulcus. Each participant completed three functional runs mapping population receptive fields (pRF) with 490 volumes per run (including 10 dummy volumes), and two functional runs for localizing face and scene regions (not reported here). A high-resolution T1-weighted MPRAGE structural scan (voxels = 1mm isotropic, TR = 2730ms, TE = 3.57ms) was also obtained for each participant.

Stimuli and Task

Each scanning session lasted approximately 1 hour. Participants lay supine with the stimuli projected onto a screen (resolution: 1920 × 1080) at the back of the bore, via a mirror mounted on the head coil. The total viewing distance was 68cm.

We used a wedge and ring stimulus containing colorful images to map participants' visual field locations. The wedge subtended a polar angle of 12° and rotated in 60 discrete steps (one per second). The maximal eccentricity of the ring was 8.5° and expanded/contracted over 36 logarithmic steps. Within reach run, there were 6 cycles of wedge rotation and 10 cycles of ring expansion/contraction, interleaved with a 30 s fixation-only period after every quarter of the run. This stimulus rotated, expanded, and contracted around a central fixation dot. The order of rotation and expansion/contraction was the same in each run. The wedge and ring apertures contained previously described natural images[5] or phase-scrambled versions thereof. Every 15 s the stimuli alternated between intact and phase-scrambled images. The sequence of individual images was pseudo-randomized. Participants were instructed to fixate at all times, and press a button if the fixation dot changed color from black to red (it could also change to a range of other colors) or if they saw a tartan pattern appear within the wedge and ring stimulus.

Pre-processing and pRF modelling

Functional MRI data were pre-processed using SPM12 (http://www.fil.ion.ucl.ac.uk/spm), MATLAB (MathWorks), and our custom SamSrf 5 toolbox for pRF mapping (https://doi.org/10.6084/m9.figshare.1344765). The first 10 volumes of each run were removed

to allow the signal to reach equilibrium. Functional images were mean bias corrected, realigned and unwarped, and co-registered to the structural scan, all using default SPM12 parameters. FreeSurfer (https://surfer.nmr.mgh.harvard.edu/fswiki) was used for automatic segmentation and reconstruction to create a 3D inflated model of the cortical from the structural scan. Functional data were projected onto the reconstructed cortical surface mesh, by sampling for each mesh vertex the time course from the nearest voxel midway between the white and grey matter surface. Linear trends were removed and time courses were *z*-normalized. The time courses of the three pRF mapping runs were averaged. Only vertices in the occipital lobe were included for further analyses, and all further analyses were performed in surface space.

Three parameters of a symmetrical, two-dimensional Gaussian pRF model were estimated for each voxel independently: x_0, y_o, and σ, where the first two denote the center coordinates of the pRF in the visual field and the third is the estimate of pRF size. The model predicted the neural response at each time point of the fMRI time course from the overlap between the pRF model and a binary mask of the visual stimulus; the resulting time course was then convolved with a canonical hemodynamic response function. We then found the combination of pRF parameters whose time course best predicted the actually observed time course. Various descriptions of the data were then derived from these parameters, including: *polar angle*, *eccentricity*, *cortical magnification factor (CMF),* and R^2 (proportion variance explained). CMF is the distance between two cortical surface points representing visual field positions 1° apart, estimated as previously described[37,38].

We conducted pRF model fitting in two stages. First, a coarse fit using an extensive grid search was performed on data smoothed with a large Gaussian kernel on the spherical surface (FWHM=5 mm). The best fitting pRF parameters were determined as those producing the maximal Pearson correlation between the predicted and actually observed fMRI time course. Then we conducted a fine fit, using parameters identified by the coarse fit on a vertex by vertex basis to seed an optimization algorithm[39,40] to minimize the sum of squared residuals between the predicted and observed time course. Only vertices whose goodness of fit on the coarse fit exceeded R^2>0.05 were included in the fine fit. This stage used the unsmoothed functional data

and also included a fourth amplitude parameter to estimate response strength. The final estimated parameter maps were then again smoothed on the spherical surface (FWHM=3 mm).

Manual delineations

Functional regions of interest were delineated manually based on polar and eccentricity maps. DSS delineated the regions of interest for the group average map on the spatially normalized cortical surface. NF and BdH delineated the retinotopic maps from individual participants in native space. BdH was blinded to the twin status of the data but both delineators showed a high level of agreement, especially for the early visual areas.

Visual regions V1, V2, V3, V3A, V3B, and V4 were manually delineated based on reversals in the polar angle map and the extent of the activated portion of visual cortex along the anterior-posterior axis. Data in regions V3A, V3B, and V4 were less consistent between delineators and across individuals, and particularly susceptible to different signal-to-noise ratios between participants. Due to their small sizes these regions are also not very suitable for the quadrant-wise analysis. Therefore, we did not analyze data from these regions further and restricted our analysis to V1-V3 only.

Spatial normalization and correlation analysis

In order to compare retinotopic maps directly across different participants, we aligned all individual surfaces to the common space of the FreeSurfer *fsaverage* template. We calculated an average retinotopic map separately for each group, MZ and DZ, respectively. Then we averaged these two group maps together into one grand mean map. This minimizes the undue influence the MZ group could have had on the average map due to its larger sample size. We then delineated visual regions V1, V2, and V3 based on this grand average retinotopic map.

We then extracted data from voxels in each visual region in the cortical template model. For each twin pair, we used voxels that surpassed a goodness-of-fit threshold of $R^2>0.1$ in the pRF model fitting, and calculated the correlation of these parameters between twins in the pair. For polar angle, we calculated a circular correlation coefficient. For eccentricity, pRF size, and CMF we calculated Spearman's rank correlation coefficient. We then averaged together the

correlation coefficients (after Fisher's z-transformation) for the MZ and DZ groups, respectively, and calculated the heritability using Falconer's formula[9] given by $H^2 = 2(M(r_{MZ}) - M(r_{DZ}))$, where $M(r_{MZ})$ and $M(r_{DZ})$ stand for the mean across correlation coefficients in the MZ and DZ groups, respectively.

Finally, we conducted statistical inference on this using a bootstrapping procedure. We resampled the two groups of twin types 10,000 times with replacement and recalculated the mean correlations and heritability for each iteration. To test whether heritability changed across visual regions, for each bootstrap iteration we further calculated a linear regression of heritability against visual region (V1, V2, and V3 dummy coded as 1, 2, and 3, respectively). The significance level of this effect was determined by the proportion of bootstrap iterations ≤0. To test if the heritability within a given visual region was significantly greater than zero, we quantified the proportion of bootstrap iterations where heritability was ≤0.

Spatial idiosyncrasies in pRF size and psychophysical measures

In order to investigate variations across the visual field, we conducted an analysis described in our previous research in which we compared psychophysical measures of size perception to pRF measures at corresponding locations in visual cortex[5]. For this we extracted pRF data that surpassed a goodness-of-fit threshold of $R^2>0.1$ in the pRF model fitting from a given visual region separately for each visual field quadrant. We then further divided these data into 1° wide eccentricity bands ranging from 0.5° to 8.5° and calculated the mean pRF size for each bin. We used a robust fit weighting each bin based on the amount of data in order to fit a linear function to each quadrant. Finally, we used these functions to determine the pRF size at 3.92° eccentricity, the location of the target stimuli in our psychophysical experiment and approximately halfway between the fovea and the peripheral edge of our retinotopic mapping stimulus. This procedure is a more robust way of estimating pRF size at a given location than simply extracting data from a particular eccentricity range because it takes all data within a visual region into account and is thus less susceptible to noise, outliers and missing data points.

We determined the heritability of these spatial idiosyncrasies by calculating the correlation across the four quadrants between twins in each pair and then comparing the

average correlation (after Fisher's z-transformation) between the MZ and DZ groups using a one-tailed t-test. We also carried out an equivalent analysis for the psychophysical measures, perceptual bias and discrimination uncertainty by calculating the correlations across quadrants between twins in each pair.

Finally, we also calculated the correlation across quadrants between perceptual biases and pRF size estimates in each individual participant, as a replication of our previous analyses[5]. Given the aim to examine the link between biases and pRF size on an individual basis, twin status is irrelevant to these analyses. We therefore pooled data across all individual participants to determine the average correlation across the entire sample. For both the quadrant-wise pRF size and perceptual measures, we used the same bootstrapping approach as described previously.

Analysis of cortical surface area

Benson delineations. Regions V1, V2, and V3 were automatically delineated using an anatomical template of human striate and extrastriate retinotopy[26]. This prediction is projected back into native space. We then extracted two metrics; absolute cortical surface area for each region of interest (cm^2) and relative surface area, that is the percentage of cortical area in a given hemisphere covered by the region of interest.

Human Connectome Project data. Processed MRI data was provided by the Human Connectome Project, including cortical surface reconstruction in individual native space. Regions V1, V2, and V3 were delineated using an anatomical template of human striate and extrastriate retinotopy[26], implemented in the neuropythy software library (https://github.com/noahbenson/neuropythy).

Acknowledgments

This research was supported by European Research Council Starting Grants 310829-WMOSPOTWU (DSS) and 852885-INDIVISUAL (BdH), as well as the Deutsche Forschungsgemeinschaft grant 222641018-SFB/TRR 135 (BdH). IA was supported by the

Medical Research Council (MR/K014382/1) and by core funding from the Wellcome Trust (203139/Z/16/Z), and JAG by the Medical Research Council (MR/K024817/1). Data were provided in part by the Human Connectome Project, WU-Minn Consortium (Principal Investigators: David Van Essen and Kamil Ugurbil; 1U54MH091657) funded by the 16 NIH Institutes and Centers that support the NIH Blueprint for Neuroscience Research; and by the McDonnell Center for Systems Neuroscience at Washington University.

Author contributions

IA: data analysis of Human Connectome Data, consultation, revised manuscript

NF: conception, study organization, data collection, initial analysis, wrote initial draft, revised manuscript

SE: data collection, study organization, initial analysis

BdH: consultation, data analysis, revised manuscript

JAG: consultation, data analysis, revised manuscript

DSS: conception, data analysis, data curation, consultation, revised manuscript

Data availability

Psychophysical and preprocessed imaging data and analysis code available at https://doi.org/10.17605/OSF.IO/Q8DRF

References

1. Russell, R., Duchaine, B. & Nakayama, K. Super-recognizers: people with extraordinary face recognition ability. *Psychon. Bull. Rev.* **16**, 252–257 (2009).
2. Witzel, C., O'Regan, J. K. & Hansmann-Roth, S. The dress and individual differences in the perception of surface properties. *Vision Res.* **141**, 76–94 (2017).
3. Afraz, A., Pashkam, M. V. & Cavanagh, P. Spatial heterogeneity in the perception of face and form attributes. *Curr. Biol. CB* **20**, 2112–2116 (2010).
4. Kosovicheva, A. & Whitney, D. Stable individual signatures in object localization. *Curr. Biol. CB* **27**, R700–R701 (2017).
5. Moutsiana, C. *et al.* Cortical idiosyncrasies predict the perception of object size. *Nat. Commun.* **7**, 12110 (2016).
6. Schwarzkopf, D. S., Song, C. & Rees, G. The surface area of human V1 predicts the subjective experience of object size. *Nat. Neurosci.* **14**, 28–30 (2011).
7. Schwarzkopf, D. S. & Rees, G. Subjective size perception depends on central visual cortical magnification in human v1. *PloS One* **8**, e60550 (2013).
8. Jansen, A. G., Mous, S. E., White, T., Posthuma, D. & Polderman, T. J. C. What twin studies tell us about the heritability of brain development, morphology, and function: a review. *Neuropsychol. Rev.* **25**, 27–46 (2015).
9. Falconer, D. S. The inheritance of liability to certain diseases, estimated from the incidence among relatives. *Ann. Hum. Genet.* **29**, 51–76 (1965).
10. Miller, S. M. *et al.* Genetic contribution to individual variation in binocular rivalry rate. *Proc. Natl. Acad. Sci. U. S. A.* **107**, 2664–2668 (2010).
11. Shannon, R. W., Patrick, C. J., Jiang, Y., Bernat, E. & He, S. Genes contribute to the switching dynamics of bistable perception. *J. Vis.* **11**, (2011).
12. Wilmer, J. B. *et al.* Human face recognition ability is specific and highly heritable. *Proc. Natl. Acad. Sci. U. S. A.* **107**, 5238–5241 (2010).
13. Zhu, Q. *et al.* Heritability of the specific cognitive ability of face perception. *Curr. Biol. CB* **20**, 137–142 (2010).
14. van Pelt, S., Boomsma, D. I. & Fries, P. Magnetoencephalography in twins reveals a strong genetic determination of the peak frequency of visually induced γ-band synchronization. *J. Neurosci. Off. J. Soc. Neurosci.* **32**, 3388–3392 (2012).
15. Muthukumaraswamy, S. D., Edden, R. A. E., Jones, D. K., Swettenham, J. B. & Singh, K. D. Resting GABA concentration predicts peak gamma frequency and fMRI amplitude in response to visual stimulation in humans. *Proc. Natl. Acad. Sci. U. S. A.* **106**, 8356–8361 (2009).
16. Gregory, S., Fusca, M., Rees, G., Schwarzkopf, D. S. & Barnes, G. Gamma Frequency and the Spatial Tuning of Primary Visual Cortex. *PloS One* **11**, e0157374 (2016).
17. Schwarzkopf, D. S., Robertson, D. J., Song, C., Barnes, G. R. & Rees, G. The frequency of visually induced γ-band oscillations depends on the size of early human visual cortex. *J. Neurosci. Off. J. Soc. Neurosci.* **32**, 1507–1512 (2012).
18. Bergmann, J. *et al.* V1 surface size predicts GABA concentration in medial occipital cortex. *NeuroImage* **124, Part A**, 654–662 (2016).

19. Cousijn, H. *et al.* Resting GABA and glutamate concentrations do not predict visual gamma frequency or amplitude. *Proc. Natl. Acad. Sci. U. S. A.* (2014) doi:10.1073/pnas.1321072111.
20. Alvarez, I., De Haas, B. A., Clark, C. A., Rees, G. & Schwarzkopf, D. S. Comparing different stimulus configurations for population receptive field mapping in human fMRI. *Front. Hum. Neurosci.* **9**, 96 (2015).
21. Dumoulin, S. O. & Wandell, B. A. Population receptive field estimates in human visual cortex. *NeuroImage* **39**, 647–660 (2008).
22. Bergmann, J., Genç, E., Kohler, A., Singer, W. & Pearson, J. Smaller Primary Visual Cortex Is Associated with Stronger, but Less Precise Mental Imagery. *Cereb. Cortex* bhv186 (2015) doi:10.1093/cercor/bhv186.
23. Bergmann, J., Genç, E., Kohler, A., Singer, W. & Pearson, J. Neural Anatomy of Primary Visual Cortex Limits Visual Working Memory. *Cereb. Cortex N. Y. N 1991* (2014) doi:10.1093/cercor/bhu168.
24. Genç, E., Bergmann, J., Singer, W. & Kohler, A. Surface Area of Early Visual Cortex Predicts Individual Speed of Traveling Waves During Binocular Rivalry. *Cereb. Cortex N. Y. N 1991* (2014) doi:10.1093/cercor/bht342.
25. Verghese, A., Kolbe, S. C., Anderson, A. J., Egan, G. F. & Vidyasagar, T. R. Functional size of human visual area V1: a neural correlate of top-down attention. *NeuroImage* **93 Pt 1**, 47–52 (2014).
26. Benson, N. C. *et al.* The Retinotopic Organization of Striate Cortex Is Well Predicted by Surface Topology. *Curr. Biol. CB* (2012) doi:10.1016/j.cub.2012.09.014.
27. Van Essen, D. C. *et al.* The WU-Minn Human Connectome Project: an overview. *NeuroImage* **80**, 62–79 (2013).
28. Glasser, M. F. *et al.* The minimal preprocessing pipelines for the Human Connectome Project. *NeuroImage* **80**, 105–124 (2013).
29. Baaré, W. F. *et al.* Quantitative genetic modeling of variation in human brain morphology. *Cereb. Cortex N. Y. N 1991* **11**, 816–824 (2001).
30. Finlayson, N. J., Papageorgiou, A. & Schwarzkopf, D. S. A new method for mapping perceptual biases across visual space. *J. Vis.* **17**, 5 (2017).
31. Silva, M. F. *et al.* Radial asymmetries in population receptive field size and cortical magnification factor in early visual cortex. *NeuroImage* **167**, 41–52 (2017).
32. Rajimehr, R. & Tootell, R. B. H. Does retinotopy influence cortical folding in primate visual cortex? *J. Neurosci. Off. J. Soc. Neurosci.* **29**, 11149–11152 (2009).
33. Van Essen, D. C. A tension-based theory of morphogenesis and compact wiring in the central nervous system. *Nature* **385**, 313–318 (1997).
34. Brainard, D. H. The Psychophysics Toolbox. *Spat. Vis.* **10**, 433–6 (1997).
35. Pelli, D. G. The VideoToolbox software for visual psychophysics: transforming numbers into movies. *Spat. Vis.* **10**, 437–42 (1997).
36. Sarna, S., Kaprio, J., Sistonen, P. & Koskenvuo, M. Diagnosis of twin zygosity by mailed questionnaire. *Hum. Hered.* **28**, 241–254 (1978).
37. Harvey, B. M. & Dumoulin, S. O. The Relationship between Cortical Magnification Factor and Population Receptive Field Size in Human Visual Cortex: Constancies in Cortical Architecture. *J. Neurosci. Off. J. Soc. Neurosci.* **31**, 13604–13612 (2011).

38. Schwarzkopf, D. S., Anderson, E. J., Haas, B. de, White, S. J. & Rees, G. Larger Extrastriate Population Receptive Fields in Autism Spectrum Disorders. *J. Neurosci.* **34**, 2713–2724 (2014).
39. Lagarias, J., Reeds, J., Wright, M. & Wright, P. Convergence properties of the Nelder—Mead simplex method in low dimensions. *SIAM J. Optim.* **9**, 112–147 (1998).
40. Nelder, J. A. & Mead, R. A Simplex Method for Function Minimization. *Comput. J.* **7**, 308–313 (1965).

Supplementary Information

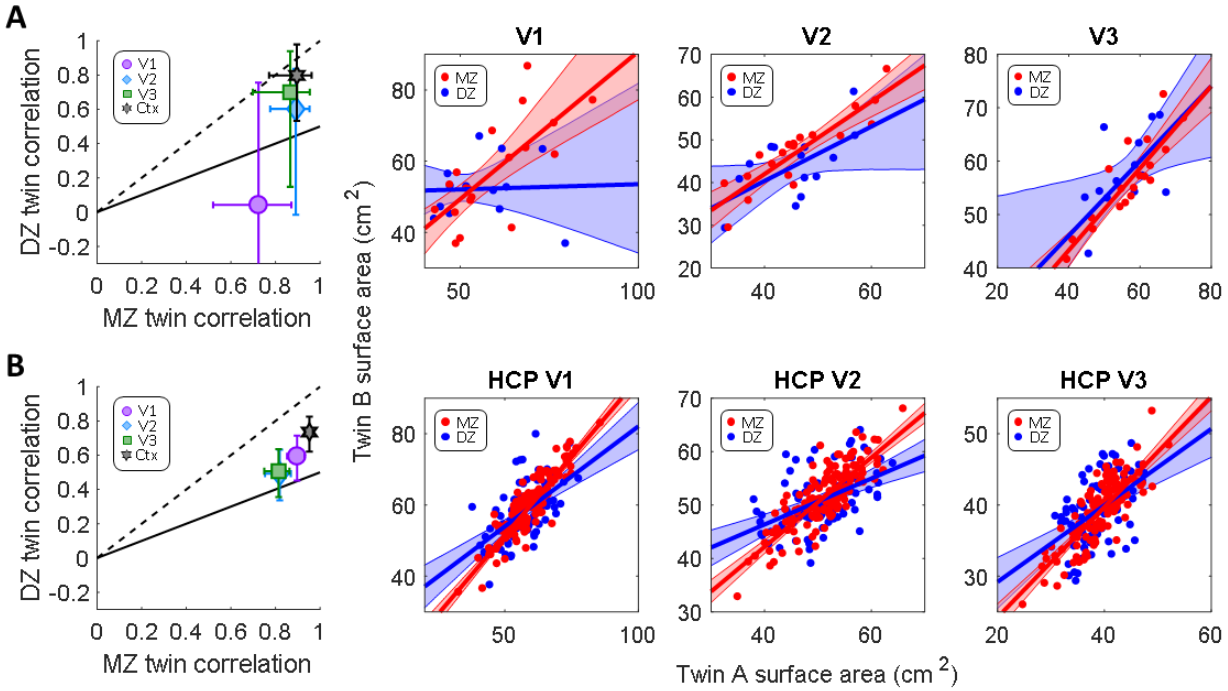

Supplementary Figure S1. *Left column:* Intra-class correlations between DZ twins plotted against that for MZ twins for absolute surface areas. Visual regions were defined based on a probabilistic anatomical procedure. Shown are data for V1 (purple disc), V2 (blue diamond), V3 (green square), and the total cortical surface area (grey hexagram). Error bars denote 95% confidence intervals based on bootstrapping. The dotted line indicates the expected correlation if a measure is only determined by shared environmental factors, the solid line if it is determined by additive genetic factors. *Other columns:* Absolute cortical surface area for regions V1-V3 for the two twins in each pair separately for the MZ (red points) and DZ (blue points) groups. Each point denotes data from one twin pair. Solid lines indicate linear regression fits for each group, and the shaded regions denote their 95% confidence intervals based on bootstrapping. A. Data from our novel sample of participants. B. Replication data from the Human Connectome Project.

Correlations for our data set: V1: r_{MZ}=0.72, p=0.0005; r_{DZ}=0.04, p=0.8849; H^2>100%. V2: r_{MZ}=0.89, p<10^{-6}; r_{MZ}=0.6, p=0.0227; H^2=58%. V3: r_{MZ}=0.87, p<10^{-5}; r_{DZ}=0.7, p=0.0054; H^2=33%. Correlations for Human Connectome Project data: V1: r_{MZ}=0.9, p<10^{-49}; r_{DZ}=0.59, p<10^{-8}; H^2=61%. V2: r_{MZ}=0.82, p<10^{-33}; r_{DZ}=0.49, p<10^{-5}; H^2=65%. V3: r_{MZ}=0.81, p<10^{-33}; r_{DZ}=0.51, p<10^{-5}; H^2=61%.

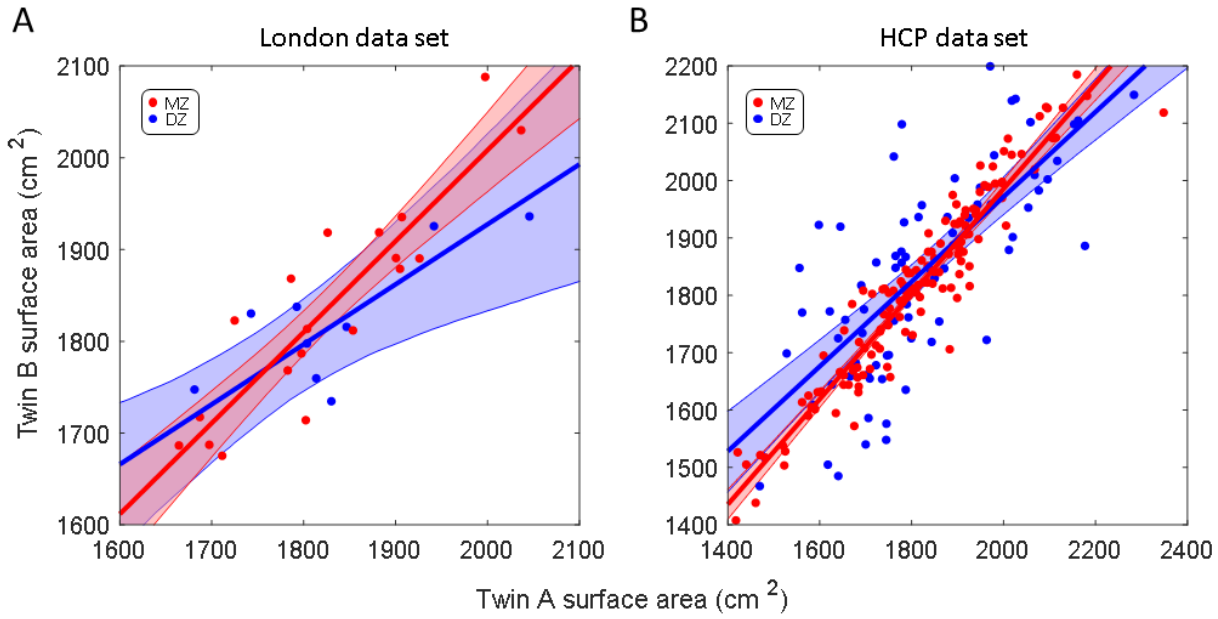

Supplementary Figure S2. Absolute surface area for the whole cortex for the two twins in each pair separately for the MZ (red points) and DZ (blue points) groups. Each point denotes data from one twin pair. Solid lines indicate linear regression fits for each group, and the shaded regions denote their 95% confidence intervals based on bootstrapping. A. Data from our novel sample of participants. B. Replication data from the Human Connectome Project.

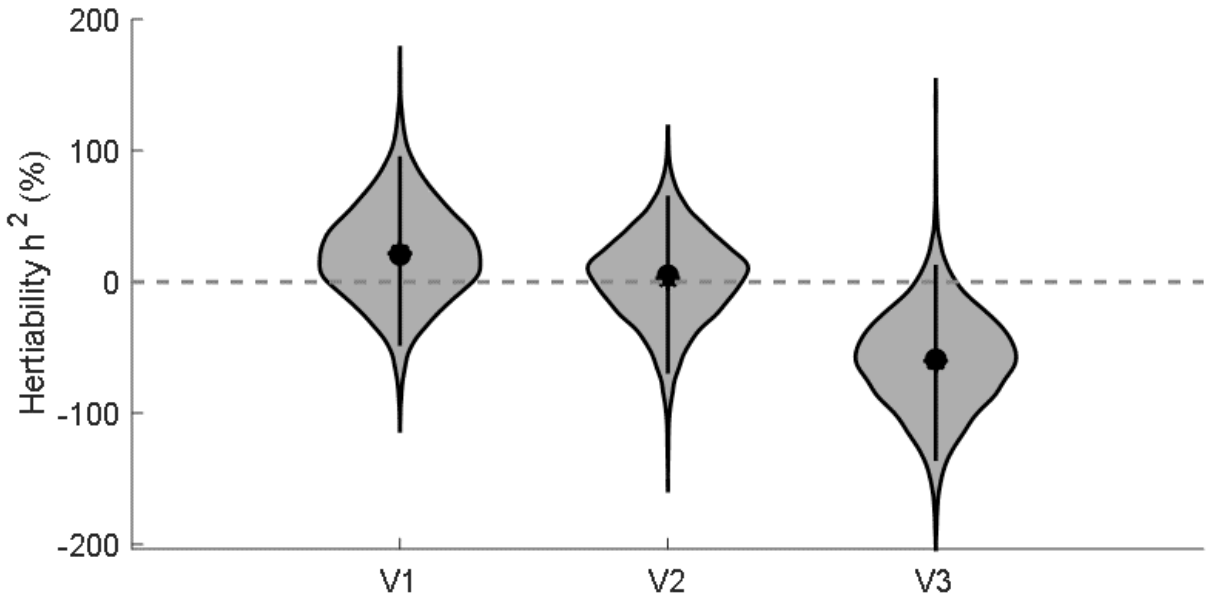

Supplementary Figure S3. Heritability for pRF size across visual field quadrants in each visual region. Filled circles indicate the group means. The violin plot shows the bootstrap distributions, and the error bars denote its 95% confidence intervals.

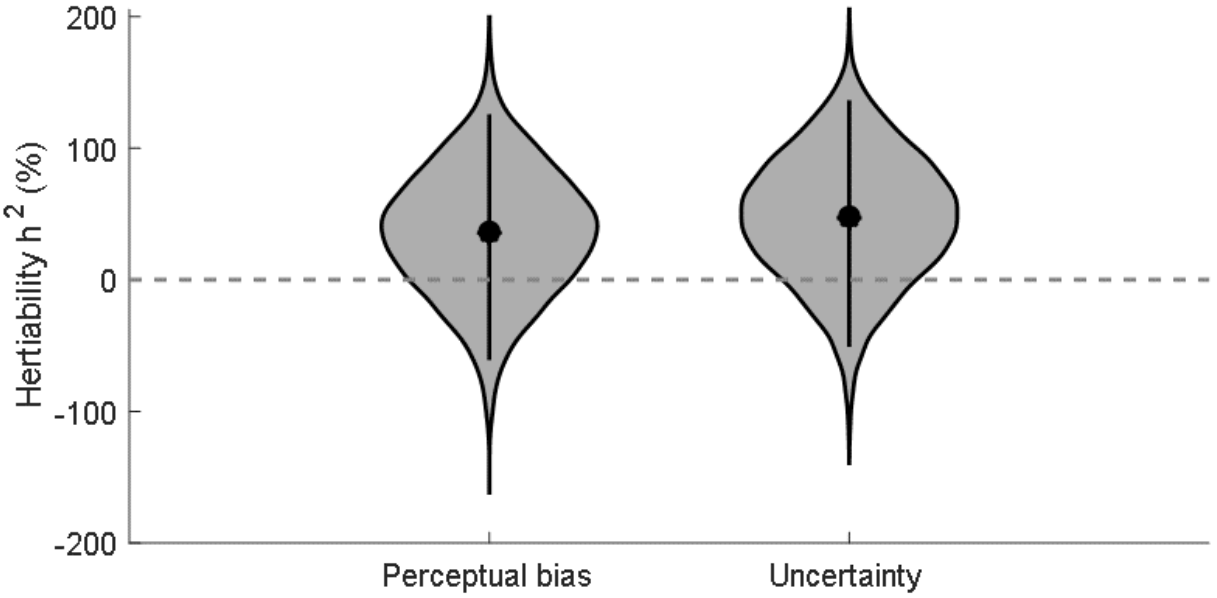

Supplementary Figure S4. Heritability for perceptual bias and discrimination uncertainty across visual field quadrants. Filled circles indicate the group means. The violin plot shows the bootstrap distributions, and the error bars denote its 95% confidence intervals.